Dielectric Properties of Human Leukocyte Subpopulations Determined by Electrorotation as a Cell Separation Criterion

Jun Yang, Ying Huang, Xujing Wang, Xiao-Bo Wang, Frederick F. Becker, and Peter R. C. Gascoyne
Department of Molecular Pathology, University of Texas MD Anderson Cancer Center, Houston, Texas 77030 USA

ABSTRACT The separation and purification of human blood cell subpopulations is an essential step in many biomedical applications. New dielectrophoretic fractionation methods have great potential for cell discrimination and manipulation, both for microscale diagnostic applications and for much larger scale clinical problems. To discover whether human leukocyte subpopulations might be separable by such methods, the dielectric characteristics of the four main leukocyte subpopulations, namely, B- and T-lymphocytes, monocytes, and granulocytes, were measured by electrorotation over the frequency range 1 kHz to 120 MHz. The subpopulations were derived from human peripheral blood by magnetically activated cell sorting (MACS) and sheep erythrocyte rosetting methods, and the quality of cell fractions was checked by flow cytometry. Mean specific membrane capacitance values were calculated from the electrorotation data as 10.5 (± 3.1), 12.6 (± 3.5), 15.3 (± 4.3), and 11.0 (± 3.2) mF/m^2 for T- and B-lymphocytes, monocytes, and granulocytes, respectively, according to a single-shell dielectric model. In agreement with earlier findings, these values correlated with the richness of the surface morphologies of the different cell types, as revealed by scanning electron microscopy (SEM). The data reveal that dielectrophoretic cell sorters should have the ability to discriminate between, and to separate, leukocyte subpopulations under appropriate conditions.

INTRODUCTION

Studies of leukocyte subpopulations often demand their separation and purification. Existing methods for accomplishing this exploit cell density (Boyum, 1974), specific immunological targets (Smeland et al., 1992), or receptor-ligand interactions (Chess and Schlossman, 1976). These methods are often inefficient and require several preparative steps involving bulky equipment such as centrifuges, large magnets, and flow cytometers. Clearly, there is a need for new sorting devices that have the capability to identify and selectively manipulate cells through novel phenomena that may introduce additional discriminatory capacity and are adaptable to automated and microfluidic applications.

Dielectrophoresis (DEP), particle motion caused by the interaction between nonuniform A.C. electrical fields and field-induced polarization in particles, has been the subject of extensive studies in recent years because it has a potential for the noninvasive separation and manipulation of biological cells according to their dielectric characteristics in both microscale and preparative applications (Washizu et al., 1990, Becker et al., 1994; Markx et al., 1994; Fuhr et al., 1996; Gascoyne et al., 1997; Huang et al., 1997). As a starting point for developing dielectrophoretic devices for hematological applications, it is critical to characterize differences in the dielectric properties of the individual human leukocyte subpopulations. A number of papers relating to the dielectric properties of human whole blood (Schwan, 1983), erythrocytes (Ballario et al., 1984), and T- or B-lymphocytes have been published (Surowiec et al., 1986; Ziervogel et al., 1986; Bordi et al., 1993; Beving et al., 1994). However, to the best of our knowledge, a comparative analysis of the dielectric properties of the major human leukocyte subtypes is not available. The purpose of this study was to determine and to compare and contrast the dielectric parameters of the major constituent subpopulations of peripheral blood, namely, T- and B-lymphocytes, granulocytes, and monocytes, and to discover whether, on the basis of differences in these parameters, these cell types should be separable by dielectrophoretic methods.

When a cell is subjected to a rotating electric field within a medium with different dielectric properties, it will start to rotate. Analysis of this so-called electrorotation (ROT) with an appropriate model allows the determination of the dielectric properties of cellular constituents for individual, intact, viable cells (Arnold et al., 1982; Fuhr et al., 1990; Gimsa et al., 1991a; Hölzel and Lamprecht, 1992; Huang et al., 1992; Wang et al., 1994). In this article, cell membrane and internal dielectric properties of T- and B-lymphocytes, monocytes, and granulocytes were characterized with single-cell discrimination in the frequency range 1 kHz to 120 MHz by ROT measurements and analyzed using a single-shell dielectric model. Scanning electron microcopy (SEM) was used to determine the relationship between the observed leukocyte dielectric properties and their membrane morphologies. Based on the dielectric parameters, size, and density characteristics found for these cells, we conclude that leukocyte subpopulations should be separable by dielectrophoretic sorters.

MATERIALS AND METHODS

Cell preparation

Human peripheral blood samples were obtained from Buffy bags (Gulf Coast Regional Blood Bank, Houston, TX) or normal healthy volunteers.

Received for publication 19 January 1999 and in final form 25 February 1999.

Address reprint requests to Dr. Xiao-Bo Wang, Department of Molecular Pathology, Box 89, University of Texas MD Anderson Cancer Center, 1515 Holcombe Boulevard, Houston, TX 77030. Tel.: 713-792-7605; Fax: 713-792-5940; E-mail: xiaobo@solace.mdacc.tmc.edu.

0006-3495/99/06/3307/08 $2.00

Cells were washed twice with Hanks' balanced salt solution (HBSS) (Irvine Scientific, Santa Ana, CA) and diluted with two to four volumes of HBSS. The granulocytes, T- and B-lymphocytes, and monocytes were separated stepwise, as illustrated in Fig. 1.

Granulocytes

After carefully overlayering four parts of blood cell suspension onto one part of Ficoll-Paque medium with a density of 1.077 g/ml (Histopaque, Sigma-Aldrich, Dorset, UK), cells were centrifuged at room temperature for 30 min at 300 × *g*. Peripheral blood mononuclear cells (PBMCs) were collected from the interface between HBSS and Histopaque gradients after centrifugation and used later for the preparation of T- and B-lymphocytes and monocytes. The cell pellet containing erythrocytes and granulocytes was then harvested. The erythrocytes in the pellet fraction were lysed in ammonium chloride lysing solution (8.26% ammonium chloride/1% potassium bicarbonate/0.037% EDTA tetrasodium), and purified granulocytes were obtained by washing twice with HBSS to remove erythrocyte debris.

T-lymphocytes

Cells from the HBSS-Histopaque interface were washed three times with HBSS, and the platelets were removed by gentle centrifugation (200 × *g* for 10 min). After washing, cells were resuspended in 30 ml RPMI 1640 supplemented with 10% fetal bovine serum (FBS), 1 mM glutamine, and 20 mM HEPES (Life Technologies, Gaithersburg, MD).

Sheep red blood cell (SRBC) rosetting was accomplished by a slight modification of the method described by Jondal et al. (1972). SRBCs (5 ml) (Colorado Serum Co., Denver, CO) were incubated with 0.1 ml neuraminidase (Calbiochem, La Jolla, CA) at 37°C for 30 min to remove erythrocyte surface charges. SRBCs were then suspended in 45 ml HBSS, centrifuged without decanting supernatant, and stored at 4°C until needed. The SRBC pellet was then withdrawn and added to PBMCs in the proportion of 0.1 ml SRBCs per 50 million PBMCs. Cells were mixed thoroughly and centrifuged for 5 min at 200 × *g* to form a soft pellet. The mixture was then incubated overnight at 4°C.

Cells were then resuspended by gentle rocking so as not to break up the T-cell-erythrocyte rosettes. After the cell suspension was brought to 40 ml with RPMI medium, 10 ml of 1.077 Histopaque was slowly layered on the bottom of the tube, and the cells were centrifuged for 30 min at 300 × *g*. B-lymphocytes and monocytes were collected at the HBSS-Histopaque interface, and T-cell-SRBC rosettes were harvested from the cell pellet at the bottom. The T-lymphocyte population was recovered from the rosettes by lysing the SRBCs with ammonium chloride solution and washing out the SRBC debris with HBSS. The recovered T-cells were then suspended in RPMI medium at the concentration of $\sim 10^6$ cells/ml.

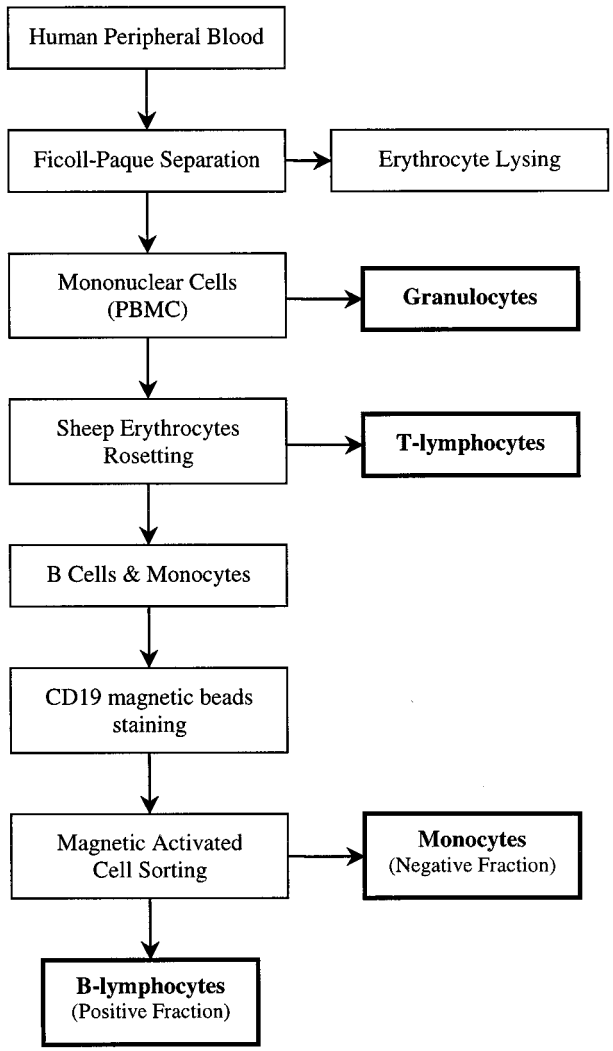

FIGURE 1 Blood cell separation procedures used in this study.

B-lymphocytes and monocytes

The combined B-cell and monocyte fraction collected from the HBSS-Histopaque interface was further processed by the superMACS high-gradient magnetic sorting system (Miltenyi Biotec, Auburn, CA). The MACS separation medium was degassed, Ca^{2+}/Mg^{2+}-free phosphate-buffered saline (PBS) (Life Technologies) supplemented with 0.5% bovine serum albumin (Sigma Chemical, St. Louis, MO) and 2 mM EDTA (Sigma Chemical) at pH 7.2. First cells were washed twice in the MACS separation medium to remove dead cells and debris. This step was found to be critical for achieving efficient separation, because it eliminated the potential not only for clumping of viable and dead cells during subsequent separation steps, but also for nonspecific binding of magnetic beads to dead cells. After washing, each 10^7 cells was suspended in 80 μl MACS separation medium and incubated at 4°C for 15 min with 20 μl CD19-conjugated magnetic beads (Miltenyi Biotec). After incubation, the cells were washed, resuspended in 1 ml MACS medium, and passed through a 30-μm nylon mesh (Miltenyi Biotec) to further remove cellular aggregates. A high-gradient magnetic VS+ type column was installed in the superMACS magnet and washed with 3 ml MACS medium before use. The cell suspension was then passed through the column, followed by four 3-ml aliquots of MACS medium to wash away unlabeled cells. The cell fraction that passed through the column without binding was composed predominately of monocytes. The B-lymphocyte fraction bound on the column by the CD19 magnetic microbeads was harvested by removing the column from the magnet and then flushing it rapidly several times with MACS separation medium.

Flow cytometry

The purity of the separated cell fractions was investigated using a Bryte HS flow cytometer system (Bio-Rad Microscience, Hercules, CA). About 10^6 cells were taken from each cell fraction, washed twice with PBS containing 2% FBS and 0.1% sodium azide (Sigma Chemical, CA), and resuspended in 50 μl of the same solution. A 20-μl reagent aliquot (Becton Dickinson, San Jose, CA) containing fluorescein isothiocyanate (FITC) or phycoerythrin (PE)-conjugated monoclonal antibodies directed against the CD3, CD20, CD14, CD15, or CD45 (leukocyte marker) antigen, or an appropriate isotype control (mouse IgG1, mouse IgG2a) was then added to the cells and incubated for 30 min at 4°C in the dark. Cells were washed again with PBS/FBS buffer and resuspended in 1 ml 1% paraformaldehyde for subsequent flow cytometry analysis. For data acquisition we used the linear amplification mode to determine forward-scatter (FCS) and side-scatter

(SSC) parameters and logarithmic amplification for fluorescence 1 (FL1 = FITC) and fluorescence 2 (FL2 = PE) parameters.

Electrorotation measurements

ROT experiments were conducted using a chamber consisting of a neoprene O-ring (15 × 1 mm) affixed with wax to a glass substrate that supported a gold polynomial electrode array with a tip-tip spacing of 400 μm, as described previously (Huang and Pethig, 1991; Huang et al., 1992; Wang et al., 1994). A rotating field was established by energizing the four polynomial electrodes with sinusoidal voltages of 0.9 V (rms) in phase quadrature. Cells were suspended in a 8.5% (w/w) sucrose/0.3% (w/w) dextrose buffer of conductivity 56 mS/m before rotation. For each ROT experiment, ~200 μl of cell suspension was pipetted into the O-ring, and a coverslip was gently pressed over its center to form a full, well-sealed chamber. After cells had settled, a round, intact cell was selected for study, and a laser tweezer (Cell Robotics, Inc., Albuquerque, NM) was used to drag it to the chamber center. ROT measurements were then made over the frequency range 1 kHz to 120 MHz at four points per decade by manually timing the cell rotation rate at each frequency by stopwatch. Two separate determinations were made of each ROT rate. Cell size was measured from the cell image on the TV monitor and calibrated against a stage micrometer. A least-squares parameter optimization method was then used to fit the single-shell dielectric model to the ROT spectra and derive the membrane-specific capacitance, internal conductivity, and permittivity for each cell, as described previously (Gimsa et al., 1991a; Wang et al., 1994; Gascoyne et al. 1995). ROT spectra for more than 30 individual cells of each leukocyte subpopulation were measured.

Scanning electron microscopy

Scanning electron microscopy (SEM) pictures were kindly taken by Kenneth Dunner, Jr., at the High Resolution Microscopy Facility, University of Texas M. D. Anderson Cancer Center. T- and B-lymphocyte, monocyte, and granulocyte cell fractions were centrifuged at 300 × g for 10 min in 15-ml conical polypropylene tubes (Becton Dickinson Labware, Lincoln Park, NJ). After the supernatant was removed, cell pellets were resuspended in 8.75% sucrose solutions for 15 min. The cells were then washed, fixed, critical-point dried, coated with Au/Pd, and studied on a Hitachi model S520 scanning electron microscope as described previously (Wang et al., 1994).

RESULTS AND DISCUSSION

Immunological typing of leukocyte subpopulations

To determine the purity of the leukocyte subpopulations derived by our separation procedures illustrated in Fig. 1 and described above, cells were labeled with either FITC or PE-conjugated CD15, CD3, CD20, or CD14 and analyzed by flow cytometer. The composition of each cell fraction was then compared with that of the starting PBMC mixture. Table 1 summarizes the compositions found for cell populations before and after purification. Mononuclear cells from the initial Ficoll-Paque gradient step contained an average of 55% T-lymphocytes, 7.5% B-lymphocytes, and 15% monocytes. Separated leukocyte populations showed an average purity of 98% (90–99%) for granulocytes, 90% (86–95%) for T-lymphocytes, 95% (90–99%) for B-lymphocytes, and 89% (86–95%) for monocytes. The high purity of each cell population enabled us to measure their dielectric properties by ROT without the need for additional cell identification methods.

TABLE 1 Percentages of leukocyte subpopulations before and after purification, as determined by flow cytometer

Cell type	Before	After
T-Lymphocytes ($CD3^+$)	55.5 ± 11.2%	89.7 ± 2.9%
B-Lymphocytes ($CD20^+$)	7.2 ± 2.0%	94.8 ± 5.1%
Monocytes ($CD14^+$)	15.6 ± 5.8%	88.9 ± 5.7%
Granulocytes ($CD15^+$)	—	97.8 ± 2.3%

ROT spectra and cell dielectric properties

Typical ROT spectra normalized against the square of the applied voltage for cells suspended in an isotonic sucrose/dextrose medium of conductivity 56 mS/m are shown in Fig. 2. Cells exhibited antifield rotation at frequencies below ~6 MHz, and above this cofield rotation occurred. The antifield peaks typically occurred at a frequency of ~200 kHz for monocytes, ~300 kHz for granulocytes, and ~350 kHz for T- and B-lymphocytes, whereas cofield peaks occurred at a frequency of ~40 MHz for all leukocyte populations.

We have previously demonstrated that cell dielectric parameters, including the specific membrane capacitance (C_{mem}), the internal conductivity (σ_{int}), and the internal permittivity (ϵ_{int}), can be derived from electrorotation spectra by an optimization procedure using a single-shell dielectric model (Wang et al., 1994). A summary of the means and standard deviations for each parameter derived from our ROT measurements is given in Table 2 for T- and B-lymphocytes, monocytes, and granulocytes. Among these cell populations, monocytes exhibited the biggest mean membrane capacitance, whereas T-lymphocytes had the

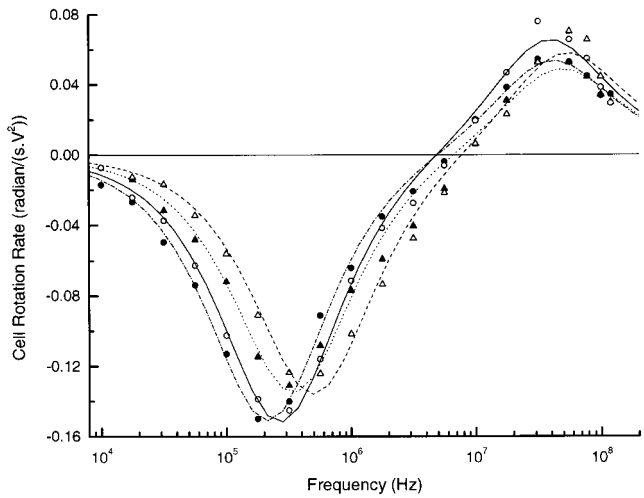

FIGURE 2 Typical ROT spectra for human peripheral blood T-lymphocytes (△), B-lymphocytes (▲), monocytes (●), and granulocytes (○) in an isotonic sucrose suspension of conductivity 56 mS/m. Continuous curves show best fits of the single-shell dielectric model (– – – for T-lymphocytes, ····· for B-lymphocytes, – · – for monocytes, and —— for granulocyes).

TABLE 2 Blood cell dielectric parameters

Cell type	Number	Radius (μm)	C_{mem} (mF/m^2)	σ_{int} (S/m)	ε_{int}
T-lymphocytes	91	3.29 ± 0.35	10.5 ± 3.1	0.65 ± 0.15	103.9 ± 24.5
B-lymphocytes	49	3.29 ± 0.26	12.6 ± 3.5	0.73 ± 0.18	154.4 ± 39.9
Monocytes	43	4.63 ± 0.36	15.3 ± 4.3	0.56 ± 0.10	126.8 ± 35.2
Granulocytes	33	4.71 ± 0.23	11.0 ± 3.2	0.60 ± 0.13	150.9 ± 39.3

smallest. Compared with T-lymphocytes, B-lymphocytes exhibited larger membrane capacitance, internal conductivity, and internal permittivity values.

Data expressing the mean membrane capacitances and mean cell radii for the leukocyte subpopulations studied are shown in Fig. 3. These reveal that monocytes and granulocytes were physically larger than lymphocytes and, for this reason, could be easily distinguished visually. For monocytes and granulocytes, the difference in membrane capacitances was significant at a confidence level of $p < 10^{-5}$, even though these two cell types had similar sizes. B- and T-lymphocytes exhibited the largest overlap in capacitance and size characteristics. Although their sizes were similar, B-lymphocytes had a slightly larger mean membrane capacitance ($p < 10^{-3}$) than T-lymphocytes. A *t*-test analysis for cell size and membrane capacitance parameters is given in Table 3.

It is important to note that the single-shell model used here to analyze the ROT spectra is an approximation of the structurally and compositionally complicated cells. For example, each cell has a nucleus that was not taken into account in the single-shell model. The consequences of using a simple model are evident in Fig. 2, where there appear to be systematic deviations between the fitted spectra and the experimental measurements in the frequency range 1–10 MHz. Although a three-shell model can provide a better fit (e.g., Fuhr et al., 1985; Gimsa et al., 1991b), the many parameters of the more complicated model cannot be determined reliably from the measured spectra (Gascoyne et al., 1995). The single-shell model adequately reflected the major features of the cell structure and provided an accurate assessment of the membrane dielectric properties in which we were most interested here. Because we use the single-shell model approximation, the dielectric parameters shown in Table 3 are effective values that apply for our experimental conditions. The suspending medium may influence these parameters, and cells may respond differently in a medium with a significantly different ionic concentration.

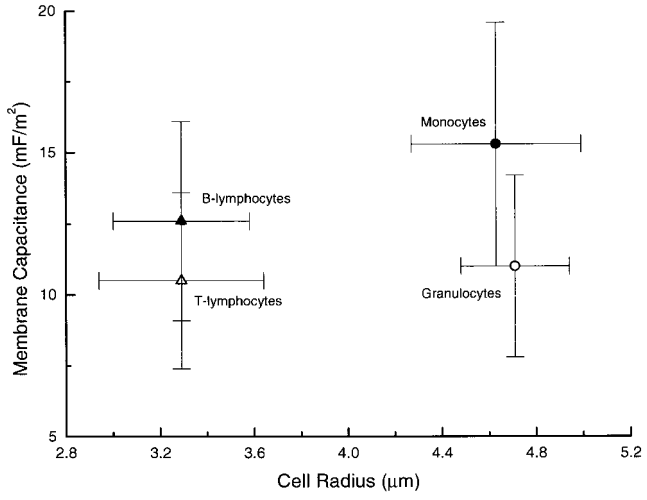

FIGURE 3 Mean and standard deviations of the specific membrane capacitances and sizes for human T-lymphocytes (△), B-lymphocytes (▲), monocytes (●), and granulocytes (○).

Cell surface morphologies

In earlier work, we showed that the membrane capacitance of cells was correlated with cell membrane area associated with membrane-rich morphological features, including folds, ruffles, and microvilli (Wang et al., 1994). To see whether this relationship also existed for leukocytes, their surface morphologies were examined by scanning electron microscope. Fig. 4 shows scanning electron micrographs for the T- and B-lymphocytes, monocytes, and granulocytes, respectively. The surface morphologies of the different blood cell types can be seen to be quite distinct.

Depicted in Fig. 4, *a* and *b*, are human T- and B-lymphocytes. These are spherical cells 6–9 μm in diameter. T-lymphocytes exhibit generally smooth surfaces, with a few projections ranging from 0.05 to 0.2 μm in length. On the other hand, B-lymphocytes appear predominately villous, exhibiting more microvilli than T-cells. The villi are 0.1 μm in diameter and range in length from 0.1 to 0.6 μm. These observations agree with earlier reports that led to the use of surface features as a criterion for distinguishing between T- and B-lymphocytes by SEM without immunologic identification (Bentwich et al., 1973; Polliack et al., 1974). However, in agreement with the observations by Bentwich et al. (1973) and Polliack et al. (1974), ~10% of the cells in our T-cell and B-cell fractions were found to have similar surface features comprising an intermediate number of microvilli. Such cells cannot be identified by SEM without a parallel immunologic assay.

Monocytes, shown in Fig. 4 *c*, are ~8–14 μm in diameter, and their surfaces are covered with well-developed and broad-based ruffles and ridge-like profiles with a general absence of microvilli. Most ruffles are 0.1 μm thick and 0.5–1 μm high and have lengths between half a micrometer and tens of micrometers. Granulocytes are shown in Fig. 4 *d*. They are about the same size as monocytes. Granulocyte membranes possess both surface projections and transverse,

TABLE 3 T-test for means of membrane capacitances and cell sizes between the paired leukocyte subpopulations

C_{mem}	T-lymphocytes	B-lymphocytes	Monocytes
Membrane capacitance			
B-lymphocytes	3.7 ($p = 3 \times 10^{-4}$)		
Monocytes	7.3 ($p < 10^{-10}$)	3.3 ($p = 2 \times 10^{-3}$)	
Granulocytes	0.8 ($p = 0.5$)	2.2 ($p = 3 \times 10^{-2}$)	4.9 ($p = 6 \times 10^{-6}$)
Cell size			
B-lymphocytes	0.1 ($p = 0.9$)		
Monocytes	20.4 ($p < 10^{-10}$)	19.7 ($p < 10^{-10}$)	
Granulocytes	21.6 ($p < 10^{-10}$)	23.6 ($p < 10^{-10}$)	1.2 ($p = 0.2$)

ridge-like profiles and ruffles. Unlike those on the monocyte surfaces, the ruffles on granulocytes are narrow and sometimes polarized toward one edge of the cells.

As evidenced in Fig. 4, individual cells within a single, purified leukocyte type may exhibit different surface morphologies. These differences may be associated with different subpopulations within a single cell type (e.g., neutrophils, eosinophils, and basophils in granulocytes or $CD4^+$, $CD8^+$ cells in T-lymphocytes). The morphological heterogeneity is reflected in the relatively large standard deviations of membrane capacitance values derived for the different leukocyte types (Table 2).

Human T- and B-lymphocytes, monocytes, and granulocytes differing in origin, appearance, and function help to defend the body against extraneous substances through a variety of mechanisms, including phagocytosis, production of cytotoxic enzymes, and antibodies (Rifkind et al., 1986). T-cells, which regulate B-cell function by helping or suppressing antibody synthesis, participate in cell-mediated immunity and may be implicated in other cell-cell interactions, whereas the principal function of B-cells is to synthesize and secrete antibodies (Rifkind et al., 1986). This could be the reason why B-cells exhibited more microvilli than most resting T-cells, because microvilli are generally regarded as a device for increasing the total surface area and thus for facilitating metabolite transport (Motta et al., 1977). Although there are some important differences, the major function of granulocytes, comprised mainly of neutrophils, and monocytes is to eliminate foreign particles by phagocytosis (Reich et al., 1993). To achieve successful destructive phagocytosis, cells must reach the site of a foreign substance, bind it, ingest it, and after a series of metabolic steps digest or destroy it (Rifkind et al., 1986). Cell membrane ruffles usually appear most at the cell surfaces. They have been observed to develop to their full height in a few minutes and then tend to migrate from the surface toward the cell interior and to surround and engulf quanta of the liquid environment as they move (Motta et al., 1977). It is not surprising, therefore, that the surfaces of granuocytes and monocytes commonly possess a greater number of ruffles.

As already discussed, previous studies have shown that cell surface morphology plays an important role in determining cell specific membrane capacitance. This is because specific membrane capacitance depends on the total membrane area of the cell, and this area increases with increasing richness in cell surface morphological features (Wang et al., 1994). The SEM pictures reveal that most B-lymphocytes have more surface features than T-lymphocytes, in accord with our dielectric analysis, which shows that their membrane capacitance is also slightly larger. Monocytes have the greatest density of folds and ruffles of the four leukocyte populations examined, and, again in agreement with the membrane area model of capacitance, their membrane capacitance is the biggest of the cell types. The only exception to this rule is granulocytes, for which the surface structure is more complicated than that of lymphocytes, whereas their specific membrane capacitances are smaller. From a physical point of view, three possible explanations could account for differences in specific membrane capacitance values observed for different cell types, namely differences in membrane area, thickness, or composition (Wang et al., 1994). It appears, therefore, that the membrane thickness or composition of granulocytes may contribute more to their membrane capacitance differences than is the case for the other leukocyte subpopulations. To summarize, human leukocyte subpopulations have different immunological functions, which may be associated with the differences in leukocyte morphology. Morphological differences, in turn, account for cell differential dielectric behaviors.

Dielectrophoretic blood cell sorters

In biological and medical applications, the purification of cell subpopulations from complex cell mixtures often forms the starting point for research protocols and the basis for clinical treatment and diagnostic protocols. In the case of human blood, the separation of functional subclasses is essential for immunological testing (Kurnick et al., 1979); highly purified cell subpopulations permit the study of signaling between blood cells (Stout, 1993) that would otherwise be impossible. Currently applied sorting technologies most frequently exploit differences in cell density (Boyum, 1974), specific immunologic targets (Smeland et al., 1992), or receptor-ligand interactions (Chess and Schlossman, 1976). These techniques are often inadequate. Sorting devices capable of identifying and selectively manipulating different cell types through novel physical properties, which offer a basis for improved sorting methodol-

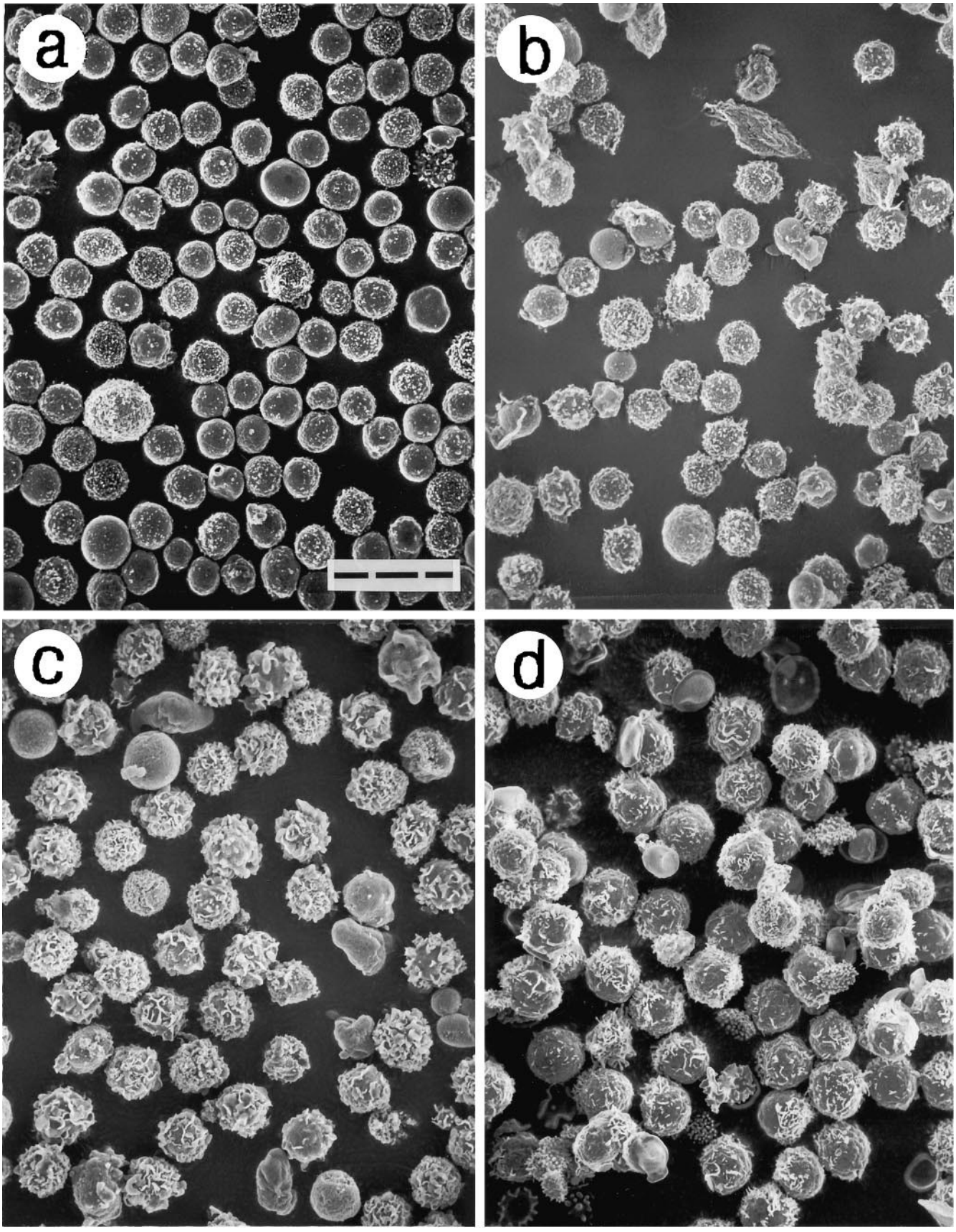

FIGURE 4 Scanning electron micrographs for human leukocytes. (*a*) T-lymphocytes. (*b*) B-lymphocytes. (*c*) Monocytes. (*d*) Granulocytes. The bar length corresponds to 20 μm.

ogies that can be used either alone or as adjuncts to existing separation techniques, are therefore desirable.

We are developing new dielectrophoretic cell sorting methods that exploit intrinsic cellular dielectric and density properties as sorting criteria. Compared with other separation methods, these offer the major advantage that cell modification with stains or antibodies or by adherence to foreign material is unnecessary, so that the potential for cell damage or activation by these probes is avoided. In addition, the dielectrophoretic sorting devices are amenable to miniaturization and integration into a complete self-contained microfluidic system for automated sorting and analysis applications.

Dielectrophoretic cell sorters utilize differences in DEP forces to discriminate between, and drive the separation of, different cell types (Becker et al., 1994, 1995; Markx et al., 1994; Gascoyne et al., 1996, 1997; Huang et al., 1997). As shown previously (Wang et al., 1995), different DEP forces result from differences between Re(f_{CM}) (the real component of f_{CM}, the Clausius-Mossotti factor) values of the different cell types. To analyze dielectrophoretic forces acting on blood cell subpopulations, we calculated the mean frequency dependencies of Re(f_{CM}) (Fig. 5) for T- and B-lymphocytes, monocytes, and granulocytes in a suspending medium of 10 mS/m, based on the mean values of their dielectric parameters derived from ROT measurement. These calculations reveal that the biggest differences in Re(f_{CM}) between different leukocyte subpopulations occur close to their DEP cross-over frequencies (the frequency at which the DEP force changes direction). For maximum discrimination, dielectrophoretic separators therefore often operate close to the frequency when Re(f_{CM}) approaches zero and where the DEP force is most sensitive to the cellular dielectric properties. The predicted DEP cross-over frequencies for B- and T-lymphocytes, monocytes, and granulocytes under the same conditions are marked on the frequency axis of Fig. 5. T- and B-lymphocytes, granulocytes, and monocytes exhibited a negative to positive DEP force transition at frequencies of ~60 kHz, ~50 kHz, ~40 kHz, and ~30 kHz, respectively, under our conditions. These frequencies are quite distinct, indicating that the separation of different leukocyte cell types by dielectrophoresis should be feasible. Two approaches have been demonstrated for dielectrophoretic separations, namely DEP retention and DEP-field flow fractionation (DEP-FFF). For DEP retention, Gascoyne et al. (1997) derived the optimum separation frequency and defined a separability factor S_{MAX} that reflects the expected differences in the DEP experienced by the two cell types to be separated. Obviously, the factor S_{MAX} depends on cell size and dielectric properties. Table 4 illustrates the application of the analysis to the leukocyte subpopulations. The biggest S_{MAX} value occurred between T-lymphocytes and monocytes, resulting from the large differences for cell radii and membrane capacitances of these two cell types. On the other hand, T- and B-lymphocytes had the smallest S_{MAX} value, because of the relatively small differences in their radii and membrane capacitances, indicating that their separation is correspondingly more difficult. Gascoyne et al. (1997) further pointed out that DEP retention method could discriminate cell types with S_{MAX} values as low as 10, suggesting that the separation of leukocyte subpopulations is possible with this method, except for the mixture of T- and B-lymphocytes and that of monocytes and granulocytes. The DEP-FFF technique has been shown to be very sensitive to cell dielectric properties when Re(f_{CM}) is close to zero (Huang et al., 1997). We are currently exploring the application of this method to separate leukocyte subpopulations.

TABLE 4 Cell separable factors* (Gascoyne et al., 1997)

C_{mem}	T-lymphocytes	B-lymphocytes	Monocytes
B-lymphocytes	3.3		
Monocyte	20.0	16.7	
Granulocyte	14.8	12.8	8.0

*Parameters are scaled by $\times 10^7$.

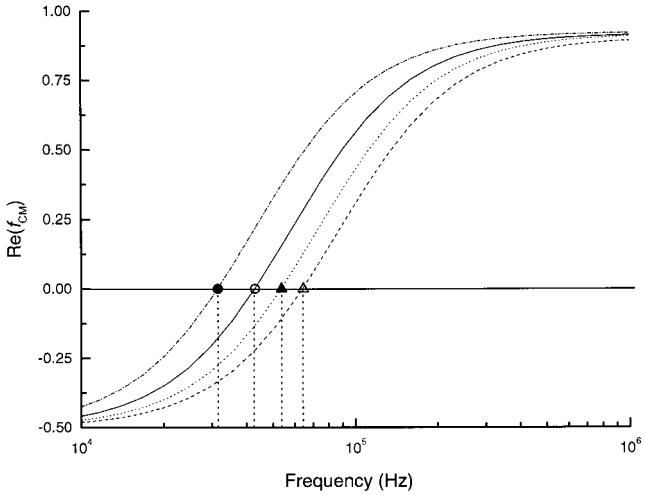

FIGURE 5 Simulated frequency dependencies of Re(f_{CM}) derived from the ROT specta for T-lymphocytes (– – –), B-lymphocytes (·····), monocytes (– · –), and granulocytes (——) in a suspending medium of 10 mS/m. Measured DEP cross-over frequencies are shown by the symbols.

We acknowledge J. Noshari and C. Joyce for cell culture and T. Anderson for techinical assistance. We also thank G. De Gasperis, K. Koo, R. Meade, and J. Vykoukal for valuable discussions.

SEM was conducted at the M. D. Anderson Cancer Center core SEM facility and supported by National Institutes of Health core grant P30-CA16672. This study is supported by National Institutes of Health grant R01 DK51065-01 from the National Institute of Diabetes and Digestive and Kidney Disease and by a contract from the Electronics Technology Office of the Defense Advanced Research Program Agency (SPAWAR Contract N66001-97-C-8608 under DARPA Order E934).

REFERENCES

Arnold, W. M., and U. Zimmermann. 1982. Rotating-field-induced rotation and measurement of the membrane capacitance of single mesophyll cells of *Avena sativa. Z. Naturforsch.* 37c:908–915.

Ballario, C., A. Bonincontro, Cametti, C., A. Rosi, and L. Sportelli. 1984. Effect of extracellular alkali metal salts on the electric parameters of human erythrocytes in normal and pathological conditions (homozygous beta-thalassemia). *Z. Naturforsch.* 39c:1163–1169.

Becker, F. F., X.-B. Wang, Y. Huang, R. Pethig, J. Vykoukal, and P. R. C. Gascoyne. 1994. The removal of human leukemia cells from blood using interdigitated microelectrodes. *J. Phys. D Appl. Phys.* 27:2659–1662.

Becker, F. F., X.-B. Wang, Y. Huang, R. Pethig, J. Vykoukal, and P. R. C. Gascoyne. 1995. Separation of human breast cancer cells from blood by differential dielectric affinity. *Proc. Natl. Acad. Sci. USA.* 92:860–864.

Bentwich, Z., S. D. Douglas, F. P. Siegal, and H. G. Kunkel. 1973. Human lymphocyte-sheep erythrocyte rosette formation: some characteristics of the interaction. *Clin. Immunol. Immunopathol.* 1:511–522.

Beving, H., L. E. Eriksson, C. L. Davey, and D. B. Kell. 1994. Dielectric properties of human blood and erythrocytes at radio frequencies (0.2–10 MHz) dependence on cell volume fraction and medium composition. *Eur. Biophys. J.* 23:207–215.

Bordi, F., C. Cametti, A. Rosi, and A. Calcabrini. 1993. Frequency domain electrical conductivity measurements of the passive electrical properties of human lymphocytes. *Biochim. Biophys. Acta.* 1153:77–88.

Boyum, A. 1974. Separation of blood leukocytes, granulocytes and lymphocytes. *Tissue Antigens.* 4:269–274.

Chess, L., and S. F. Schlossman. 1976. Anti-immunoglubulin columns and the separation of T, B, and null cells. *In* In Vitro Methods in Cell Mediated and Tumor Immunity. B. R. Bloom and J. R. David, editors. Academic Press, New York. 255–261.

Fuhr, G., J. Gimsa, and R. Glaser. 1985. Interpretation of electrorotation of protoplasts. I. The theoretical considerations. *Stud. Biophys.* 108: 149–164.

Fuhr, G., P. Rösch, T. Müller, V. Dressler, and H. Göring. 1990. Dielectric spectroscopy of chloroplasts isolated from higher plants—characterization of the double-membrane system. *Plant Cell Physiol.* 31:975–985.

Fuhr, G., U. Zimmermann, and S. G. Shirley. 1996. Cell motion in time-varying fields: principle and potential. *In* Electromanipulation of Cells. U. Zimmermann and G. A. Neil, editors. Chemical Rubber Co. Press, Boca Raton, FL. 259–328.

Gascoyne, P. R. C., F. F. Becker, and X.-B. Wang. 1995. Numerical analysis of the influence of experimental conditions on the accuracy of dielectric parameters derived from ROT measurements. *Bioelectrochem. Bioenerg.* 36:115–125.

Gascoyne, P. R. C., Y. Huang, X.-J. Wang, J. Yang, G. DeGasperis, and X.-B. Wang. 1996. Cell separation by conventional dielectrophoresis combined with field-flow fractionation. *Biophys. J.* 70:A333.

Gascoyne, P. R. C., X.-B. Wang, Y. Huang, and F. F. Becker. 1997. Dielectrophoretic separation of cancer cells from blood. *IEEE Trans. Ind. Appl.* 33:670–678.

Gimsa, J., R. Glaser, and G. Fuhr. 1991a. Theory and application of the rotation of biological cells in rotation electric fields. *In* Physical Characterization of Biological Cells. W. Schutt, H. Klinkmann, I. Lamprecht and T. Wilson, editors. Gesundheit, Berlin. 295–323.

Gimsa, J., P. Marszalek, U. Loewe, and T. Y. Tsong. 1991b. Dielectrophoresis and electrorotation of neurospora slime and murine myeloma cells. *Biophys. J.* 60:749–760.

Hölzel, R., and I. Lamprecht. 1992. Dielectric properties of yeast cells as determined by ROT. *Biochim. Biophys. Acta.* 1104:195–200.

Huang, Y., R. Hölzel, R. Pethig, and X.-B. Wang. 1992. Differences in the AC electrodynamics of viable and non-viable yeast cells determined through combined dielectrophoresis and ROT studies. *Phys. Med. Biol.* 37:1499–1517.

Huang, Y., and R. Pethig. 1991. Electrode design for negative dielectrophoresis. *Meas. Sci. Technol.* 2:1142–1146.

Huang, Y., X.-B. Wang, F. F. Becker, and P. R. C. Gascoyne. 1997. Introducing dielectrophoresis as a new force field for field-flow fractionation. *Biophys. J.* 73:1118–1129.

Jondal, M., G. Holm, and H. Wigzell. 1972. Surface markers on human T and B lymphocytes. I. A large population of lymphocytes forming nonimmune rosettes with sheep red blood cells. *J. Exp. Med.* 136: 207–215.

Kurnick, J. T., L. Östberg, M. Stegagno, A. K. Kimura, A. Örn, and O. Sjöberg. 1979. A rapid method for the separation of functional lymphoid cell populations of human and animal origin on PVP-silica (Percoll) density gradients. *Scand. J. Immunol.* 10:563–573.

Markx, G. H., M. Talary, and R. Pethig. 1994. Separation of viable and non-viable yeast using dielectrophoresis. *J. Biotechnol.* 32:29–37.

Motta, P., P. M. Andrews, and K. R. Porter. 1977. Microanatomy of Cell and Tissule Surfaces: An Atlas of Scanning Electron Microscopy. Lea and Febiger, Philadelphia. 1–11.

Polliack, A., S. M. Fu, S. D. Douglas, Z. Bentwich, N. Lampen, and E. De Harven. 1974. Scanning electron microscopy of human lymphocyte sheep erythrocyte rosettes. *J. Exp. Med.* 140:146–158.

Reich, P. R., E. K. Marshall, and F. W. Peter. 1993. Leukocytes. *In* Hematology Pathophysiologic Basis for Clinical Practice. S. H. Robinson and P. R. Reich, editors. Little, Brown and Co., Boston, Toronto, and London. 229–263.

Rifkind, R. A., A. Bank, P. A. Marks, K. L. Kaplan, R. R. Ellison, and J. Lindenbaum. 1986. Fundamentals of Hematology. Year Book Medical Publishers, Chicago and London. 94–107.

Schwan, H. P. 1983. Electrical properties of blood and its constituents: alternating current spectroscopy. *Blut.* 46:185–197.

Smeland, E. B., S. Funderud, H. K. Blomhoff, and T. Egeland. 1992. Isolation and characterization of human hematopoietic progenitor cells: an effective method for the positive selection of CD34(+) cells. *Leukemia.* 6:845–852.

Stout, R. D. 1993. Macrophage activation by T cells: cognate and non-cognate signals. *Curr. Opin Immunol.* 5:398–403.

Surowiec, A., S. S. Stuchly, and C. Izaguirre. 1986. Dielectric properties of human B and T lymphocytes at frequencies 20 kHz to 100 MHz. *Phys. Med. Biol.* 31:43–53.

Wang, X.-B., Y. Huang, P. R. C. Gascoyne, F. F. Becker, R. Hölzel, and R. Pethig. 1994. Changes in Friend murine erythroleukaemia cell membranes during induced differentiation determined by ROT. *Biochim. Biophys. Acta.* 1193:330–344.

Wang, X.-B., M. P. Hughes, Y. Huang, F. F. Becker, and P. R. C. Gascoyne. 1995. Non-uniform spatial distributions of both the magnitude and phase of AC electric fields determine dielectrophoretic forces. *Biochim. Biophys. Acta.* 1234:185–194.

Washizu, M., T. Nanba, and S. Masuda. 1990. Handling biological cells using a fluid integrated circuit. *IEEE Trans. Ind. Appl.* 26:352–358.

Ziervogel, H., R. Glaser, D. Schadow, and S. Heymann. 1986. Electrorotation of lymphocytes—the influrence of membrane events and nucleus. *Biosci. Rep.* 6:973–982.